The Cryosphere Discuss., https://doi.org/10.5194/tc-2017-121
Manuscript under review for journal The Cryosphere
Discussion started: 17 July 2017

The Cryosphere Discussions
Open Access
EGU

Simulating ice thickness and velocity evolution of Upernavik Isstrøm 1849–2012 by forcing prescribed terminus positions in ISSM

Konstanze Haubner[1,2], Jason E. Box[1], Nicole J. Schlegel[3,4], Eric Y. Larour[3], Mathieu Morlighem[5], Anne M. Solgaard[1], Kristian K. Kjeldsen[6], Signe H. Larsen[1,7], and Kurt H. Kjær[2]

[1]Geological Survey of Denmark and Greenland (GEUS), Copenhagen, Denmark
[2]Centre for GeoGenetics, Natural History Museum, University of Copenhagen, Copenhagen, Denmark
[3]Jet Propulsion Laboratory (JPL), California Institute of Technology, Pasadena, CA, USA
[4]University of California, Los Angeles, CA, USA
[5]Department of Earth System Science, University of California-Irvine, Irvine, CA, USA
[6]DTU Space - National Space Institute, Technical University of Denmark, Department of Geodesy, Kgs. Lyngby, Denmark.
[7]Centre for Ice and Climate, Niels Bohr Institute, University of Copenhagen, Copenhagen, Denmark

Correspondence to: Konstanze Haubner (khu@geus.dk)

Abstract. Tidewater glacier velocity and mass balance are sensitive to terminus retreat. Yet, it remains challenging for ice flow models to reproduce observed ice marginal changes. Here, we simulate the 1849–2012 ice velocity and thickness changes on Upernavik Isstrøm using the Ice Sheet System Model (ISSM; Larour et al., 2012), by prescribing observed glacier terminus changes. We find that a realistic ISSM simulation of the past mass balance and velocity evolution of Upernavik Isstrøm is highly dependent on terminus retreat. At the end of the 164 year simulation, the 1990–2012 ice surface elevation and velocities and are within ±20 % of the observations. Thus, our model setup provides a realistic simulation of the 1849–2012 evolution for Upernavik Isstrøm. Increased ice flow acceleration is simulated during the 1930s, late 1970s and between 1995 and 2012, coinciding with increased prescribed negative surface mass balance anomalies and terminus retreat. The simulation suggests three distinct periods of mass change: (1849–1932) having near zero mass balance, (1932–1992) with ice mass loss dominated by ice dynamical flow, and (1998–2012), where increased retreat and negative surface mass balance anomalies lead to mass loss twice that of any earlier year. The main products resulting from this study are 1849–2012 reconstruction of surface elevation, velocity and grounding line position of Upernavik Isstrøm.

1 Introduction

In recent decades, glaciers terminating into the ocean (tidewater glaciers) show increasing melt rates and acceleration (e.g. Pritchard et al., 2009; Rignot et al., 2011; Velicogna et al., 2014; Khan et al., 2015). Increased air and ocean temperatures induce increased surface melt rates and frontal retreat (Podrasky et al., 2012; Rosenau et al., 2013; Moon et al., 2014), represented by submarine melt and iceberg break-off (calving). The Greenland ice sheet consists of more than 240 tidewater glaciers (Rignot and Mouginot, 2012) and its mass balance is highly affected by changes in tidewater glacier discharge (van den Broeke et al., 2009; Bevan et al., 2012; McMillan et al., 2016). Global sea level is influenced by Greenland's ice mass changes (e.g. Rignot et al., 2011; Gardner et al., 2013) and sea level projections rely on models to estimate discharge and Greenland's contribution

to sea level. However, ice flow models still do not fully reproduce observed changes in calving front retreat and ice flow speed (Nick et al. (2009), IPCC, 2013 chapter 13).

Tidewater glacier retreat occurs due to calving (Benn et al., 2007; Nick et al., 2010) and submarine frontal melt (Motyka et al., 2011; O'Leary and Christoffersen, 2013; Morlighem et al., 2016a; Rignot et al., 2016). Yet, no universal calving law exists (Benn et al., 2007) and model approaches either (1) focus on the development and performance of a particular calving law (e.g. Cook et al., 2014; Todd and Christoffersen, 2014); (2) simplify the glacier simulation using flow line or flow band models (e.g. Nick et al., 2013; Lea et al., 2014), neglecting e.g. across-flow stresses or (3) are too complex and not well suited for long-term studies (Åström et al., 2013, 2014).

Upernavik Isstrøm (UI), a set of West Greenland tidewater glaciers, has been the focus of several observational studies. Weidick (1958) compiled historical records of UI terminus positions between 1849 and 1953, concluding that terminus retreat had increased starting in the 1930s. Observed periods of increased UI terminus retreat in 1931 to 1946, in the late 1990s and in 2005–2009 correlate with elevated air temperatures (Andresen et al., 2014). Two dynamic ice loss events took place on UI between 1985–2010 (Kjær et al., 2012) and were responsible for 80 % of the ice mass loss during 1985–2012 (Khan et al., 2013). Hence, previous studies either simulate tidewater glacier retreat with ice flow models or discuss observed terminus changes and its implications for tidewater glaciers.

In this study, we combine observations and ice flow models by using observed terminus positions in the Ice Sheet System Model (ISSM; Larour et al., 2012) to simulate Upernavik's glacial system evolution from 1849, near the end of the Little Ice Age, to 2012. We reconstruct the 1849 ice surface elevation and force ISSM glacier terminus retreat with 27 observed terminus positions.

This study does not aim to simulate physically caused retreat, instead we evaluate the effects of changing termini on UI's ice surface elevation and velocity. We (1) investigate whether prescribed terminus change produces a realistic thinning and velocity history; (2) compare simulated mass loss, surface elevation and velocity changes with 1985–2012 observations; and (3) correlate the calculated dynamic ice loss with observational studies. ISSM produces a monthly reconstruction of UI ice elevation, grounding line position, and surface velocity from 1849–2012.

2 Area and Data

UI has a catchment area of 64,667 km^2, terminating into several tidewater glaciers. We denote three main glaciers by UI-1, UI-2 and UI-3 from north to south (Fig. 1). Historically, the three glaciers shared the same terminus between 1849 and 1931 (Fig. 1; Weidick (1958)). In the 1930s the glaciers separated in two, UI-1/UI-2 and UI-3. UI-1 and UI-2 decoupled after 1966. Historical front positions (Fig. 1) were collected from several sources: 1849–1953 (historical records; Weidick, 1958), 1966–1975 (satellite images; Andresen et al., 2014), 1985–1996 (aerial photographies (1985) and satellite images; Khan et al., 2013), 1999 to 2012 (satellite images; Jensen et al., 2016).

For initialisation and evaluation of the model we use data from other studies, described in table 1.

The Cryosphere Discuss., https://doi.org/10.5194/tc-2017-121
Manuscript under review for journal The Cryosphere
Discussion started: 17 July 2017

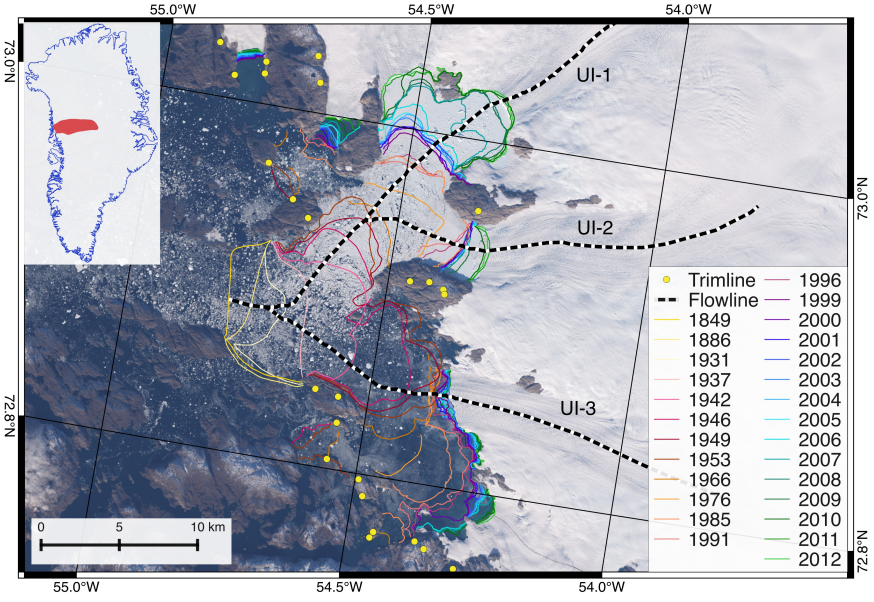

Figure 1. Upernavik Isstrøm's observed margin front positions between 1849 and 2012 (lines) and trimline positions (yellow dots; Kjeldsen et al., 2015). The background image is from Landsat 8 (September 2013). Inset is the Upernavik catchment (red area), defined by 2008/09 surface velocity from Rignot and Mouginot (2012)

3 Ice Flow Model

We use the Ice Sheet System Model (ISSM; Larour et al., 2012), a finite-element thermomechanical ice flow model. Ice flow is calculated applying the Shelfy Stream Approximation (SSA; MacAyeal, 1989), using vertically averaged ice properties (e.g. rheology, thickness, velocity). SSA is a 2-D approximation of the 3-D Stokes equation with the ability of upstream ice pushing downstream by including the effects of longitudinal stress and neglecting lateral drag.

Ice viscosity is given by Glen's Flow law (Cuffey and Paterson, 2010), with temperature dependent, spatially varying ice viscosity parameter B, calculated by applying the 1964–1990 UI mean surface air temperature (Box, 2013) to table 3.4 in Cuffey and Paterson (2010, p. 75). The mean time period is chosen, since surface air temperature and SMB are stable on UI during 1964–1990. The mesh has a resolution that varies between 300–800 m in the area of observed terminus changes and 12 km near the ice divide, resulting in about 17,000 mesh elements. Resolution increases with larger changes in ice velocity (Rignot and Mouginot, 2012) or bedrock topography (Morlighem et al., 2016b) and decreases stepwise with distance from the front.

The Grounding line position is automatically calculated in each simulation time step (Seroussi et al., 2014). We impose hydrostatic pressure at the terminus and keep the ice velocity and surface elevation constant at the inland boundary, setting ice surface velocity to the 2008/09 observed velocity (Rignot and Mouginot, 2012) and setting ice surface elevation to the GIMP

The Cryosphere Discuss., https://doi.org/10.5194/tc-2017-121
Manuscript under review for journal The Cryosphere
Discussion started: 17 July 2017

Table 1. Data for initializing and evaluating the simulation

Datum	Source	Description
Bed topography	Morlighem et al. (2016b)	derived with mass conservation approach, extended with bathymetry measurements
Bathymetry measurement		2012 NASA project, led by Eric Rignot and Todd Dupont
Bathymetry measurement	Fenty et al. (2016); OMG Mission. (2016)	NASA project Oceans Melting Greenland OMG
Bathymetry measurement	Andresen et al. (2014)	ship-based single point echo sounders
Trim line points	Kjeldsen et al. (2015)	Little Ice Age maximum extent (Fig. 1)
Surface mass balance (SMB)	Box (2013)	monthly data, covering 1840–2012
1985 Digital elevation model (DEM)	Korsgaard et al. (2016)	based on aerial photographs, 25 m resolution
2005 DEM	Howat and Eddy (2011)	Greenland Ice Sheet Mapping Project (GIMP), 30 m resolution
2012 DEM	Noh and Howat (2015)	ArcticDEM, 2–10 m resolution
Ice surface velocity	Rignot and Mouginot (2012)	winter 2008/09
Ice surface velocity	Nagler et al. (2017)	provided by ESA project Climate Change Initiative (CCI) in winters between 1991/92 and 2008/09
Ice surface velocity	Howat (2016)	provided by MEaSUREs, in the winters 2000/01, 2007/08 and 2009/10
Ice surface elevation	Thomas and Studinger (2010); Krabill (2010, updated 2016)	from IceBridge ATM; UI-1 in 2009–2012 and UI-3 in 1994, 1999, 2002, 2009, 2010, 2012
Mass change	Wiese et al. (2015); Watkins et al. (2015)	provided by the Jet Propulsion Laboratory (version: JPL RL05M GRACE mascon solution); suitable for regional (300 km scale) ice sheet mass change comparisons (Schlegel et al., 2016)

DEM (Howat et al., 2014). No submarine frontal melt or calving rates are applied, since the study aims to simulate ice velocity and thickness changes caused by observational prescribed terminus changes.

3.1 Model Initialisation

Since starting the simulation in 1849 extends the present day ice extent by 356 km^2, model initialisation requires reconstruction of both the ice surface elevation and ice velocities in the extended area. To initialise the model we thus reconstruct the 1849 ice surface elevation and velocity, described in the following. Over the present day ice covered area, ISSM is initialised with 2008/09 ice surface velocity (Rignot and Mouginot, 2012) and 2005 ice surface elevation (GIMP; Howat et al., 2014). The present day ice surface velocity is extended to the 1849 ice extent along the flow lines, following fjord bathymetry. Away from

The Cryosphere Discuss., https://doi.org/10.5194/tc-2017-121
Manuscript under review for journal The Cryosphere
Discussion started: 17 July 2017

the flow lines, missing velocity values are extrapolated. At the 1849 terminus, the ice surface elevation is set to 70 m a.s.l. consistent with marine termini in the area, based on IceBridge data (Krabill, 2010, updated 2016). Trimline data points (Fig. 1; Kjeldsen et al., 2015) mark the 1849 surface elevation and ice extent along the fjords. In the remaining area the ice surface elevation is interpolated. Given the new ice surface and the floatation criterion (Cuffey and Paterson, 2010):

$$h_{float} = \frac{\rho_{water}}{\rho_{ice}} h_{water}, \quad (1)$$

with ocean water density $\rho_{water} = 1,023\,\mathrm{kg\,m^{-3}}$, ice density $\rho_{ice} = 917\,\mathrm{kg\,m^{-3}}$ and the water depth h_{water}, we calculate the ice shelf floatation height h_{float}. Thus, the ice thickness is set to h_{float} or to the maximum thickness, defined through the initialized ice surface elevation and bed topography.

As we are interested in determining how the model geometry and velocity react to the prescribed terminus change and not internal model instability, we relax the model prior to the transient run, bringing ice surface elevation and velocity into equilibrium (following Schlegel et al. (2016)). Equilibrating model geometry and velocity requires constant forcing, i.e. a stable SMB. The SMB at Upernavik is found to be stable in 1854–1900 and 1964–1990. The mean 1854–1900 SMB value is used for equilibrating the model for 1849 conditions and 1964–1990 is set as the SMB reference period to evaluate simulated mass balance.

We perform two successive relaxations to equilibrate the model stepwise, each relaxation starting from previous relaxed model applying the 1854–1900 mean SMB. The first relaxation recalculates ice surface elevation and velocity constrained by ice flow equations implemented in ISSM, to minimise inconsistencies between reconstructed ice surface elevation and velocity, resulting from data interpolation onto the mesh and extrapolation. The basal friction coefficient for the first relaxation is chosen so that the driving stress is balanced by basal drag at any given point.

The first relaxation is stopped after 125 years simulation and provides ice thickness and velocity for the second relaxation. Given computed ice velocity from the first relaxation, basal friction can be redefined. The Basal friction coefficient is constant in time, but varies in space, and is calculated by an adjoint-based inversion, following Morlighem et al. (2010) and MacAyeal (1993), minimising the error between the observed velocity and the simulated velocity.

The second relaxation runs for 5,000 years until ice velocity and thickness are equilibrated. The end state of this relaxation provides the initial values of simulated ice thickness, surface velocity and pressure at the bed for the 1849–2012 simulations.

3.2 Simulation Setup

We run two different model simulations: (1) a control run $\mathrm{ISSM_{control}}$, forced only by monthly SMB (Box, 2013) using a fixed terminus at the observed 1849 ice margin and (2) a prescribed terminus change simulation $\mathrm{ISSM_{PT}}$, forced by monthly SMB and observed calving front positions. $\mathrm{ISSM_{control}}$ serves to estimate the ice mass, velocity and surface elevation changes that are simulated without prescribed terminus change.

The prescribed terminus position change in $\mathrm{ISSM_{PT}}$ is implemented through a levelset based method (Bondzio et al., 2016, 2017) and performed in July of the observation year, according to observed terminus positions (Fig. 1). The highest surface air temperatures and melt rates on UI are observed in July, increasing the likelihood of terminus retreat (van As et al., 2016).

The Cryosphere Discuss., https://doi.org/10.5194/tc-2017-121
Manuscript under review for journal The Cryosphere
Discussion started: 17 July 2017

We introduce 20 additional calving front positions, linearly interpolated between the observed termini and constrained by the mesh resolution to reduce induced ice area changes that are causing numerical instabilities in the ice flow equations.
The simulation evaluation time step is set to 73 h, constrained by the CFL condition (Courant et al., 1967), ensuring the numerical stability solving the ice flow equations at each time step.

4 Results and Comparison

During the simulation, most of the ice surface elevation and velocity changes occur near the central flow lines of UI-1, UI-2 and UI-3. Elevation and velocity changes in the majority of the model domain (more than 70 km inland or 5 km away form the central flow lines of the three glaciers) are below 2 %, corresponding to below 20 m and 10 m y^{-1} changes. Hence, in the following we present relative and absolute changes in ice velocity and surface elevation along the central flow lines of UI-1, UI-2 and UI-3 (from the 2012 terminus reaching 30 km upstream; Fig. 1).

4.1 Model comparison

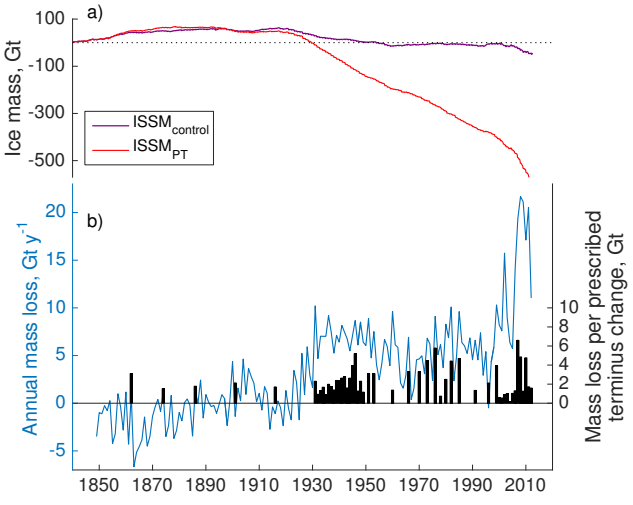

Figure 2. a) Simulated cumulative ice mass in Gt. $ISSM_{PT}$ changes are shown in red; control run changes in purple. b) The blue curve illustrates simulated annual ice loss for $ISSM_{PT}$. The black bars indicate the ice mass that is removed due to prescribed change of the terminus position.

Between 1849 and 2012, $ISSM_{control}$ shows less than 7 % surface elevation lowering and 6 % acceleration, simulating a change in velocity less than 120 m y^{-1} and a surface elevation lowering less than 10 m along the central flow lines for the entire period. In contrast, $ISSM_{PT}$ produces on average 36 % elevation lowering in 1849–2012, reaching up to 84 % at the 2012 UI-2 terminus. The average ice surface velocity increase along UI-1 and UI-2 is 180 % and on UI-3 is 47 %. Cumulative ice mass loss over the simulation period of the entire model domain (converted from modelled water equivalent assuming

The Cryosphere Discuss., https://doi.org/10.5194/tc-2017-121
Manuscript under review for journal The Cryosphere
Discussion started: 17 July 2017

917 kg m^{-3} ice density) was by the end of the model simulation −45 Gt for ISSM$_{control}$ and −585 Gt for ISSM$_{PT}$ (Fig. 2). The following section focuses on presenting ISSM$_{PT}$ results in more detail.

4.2 Mass balance

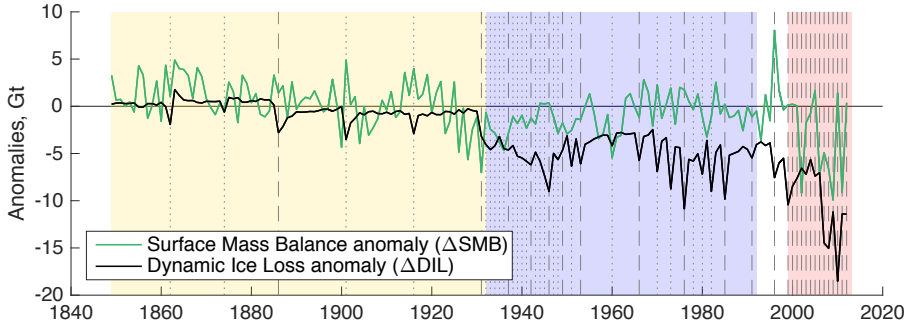

Figure 3. Simulated ice mass changes from anomalies (relative to 1964–1990 mean values) for the simulation ISSM$_{PT}$. The background is highlighted in yellow for periods of time where ΔSMB controlled MB, blue is where ice mass loss is driven by ΔSID and red, where ΔSMB and ΔSID have equally increased influence on the MB. Prescribed termini changes are marked with dashed (observations) and dotted (interpolation) lines.

In the following section we focus on the simulated mass balance (MB) through the model runs (see cumulated mass change in Fig. 2). For tidewater glaciers, mass balance can be attributed to either changes in SMB or changes in dynamic ice loss (DIL). A tidewater glacier is in equilibrium, when SMB and DIL are in balance. Deviations in SMB and DIL change the glacier and its stability, hereafter anomalies ΔSMB and ΔDIL. SMB is a model input and ΔSMB are calculated relative to the mean value of the stable UI period 1964–1990 SMB. ΔDIL is calculated as the residual between the simulated MB and ΔSMB.

The simulated annual MB for the UI catchment (Fig. 2) is positive from 1849 to 1920. In this period, the MB from the ISSM$_{PT}$ and ISSM$_{control}$ are similar due to very few and small terminus changes (Fig. 2) and MB is thus dominated by ΔSMB. Anomalies in DIL (Fig. 3) are evident by small (−0.5 to −4 Gt) peaks that coincide with prescribed terminus retreat. After 1920, the MB becomes negative, except in 1996, when ΔSMB has a peak (8 Gt), which is attributed to a high winter accumulation (McConnell et al., 2001; Box et al., 2006). Figure 3 highlights three periods in MB trends: (1) 1849–1932, when MB is close to zero, (2) from 1932 to 1992, when the negative total MB is driven by ΔDIL, and (3) 1998–2012, when SMB and DIL both have high negative anomalies and the total mass loss each year is twice as high as any year before.

Simulated mass changes in 1985–2002/05 and 2009–2011 correspond with observed mass changes from Kjær et al. (2012); Khan et al. (2013) and Larsen et al. (2016) (Table 2). In 2002/05–2010 and 2000–2005, simulated mass changes are 85 % larger than the maximum of what is observed. DIL is 85 % the mass change from 1985–2010. During 2000 to 2005 DIL is 85 % the mass change and in 2006–2011 the DIL is 60 % of mass changes, in agreement with Khan et al. (2013) and Larsen et al. (2016).

The Cryosphere Discuss., https://doi.org/10.5194/tc-2017-121
Manuscript under review for journal The Cryosphere
Discussion started: 17 July 2017

Table 2. Observed vs. simulated mass changes (with $ISSM_{PT}$)

	Khan et al. (2013)[a]		Larsen et al. (2016)		
	$1985-2002/05$	$2002/05-2010$	$2000-2005$	$2006-2008$	$2009-2011$
Observed changes, Gt	-32 ± 9	-17 ± 10	-6 ± 20	-25 ± 14	-39 ± 17
Simulated changes, Gt	-37 [b]	-32 [b]	-48	-41	-44

[a] converted from km^3 to Gt ice equivalent
[b] results from $2002/05$ as mean values of that time

A comparison with GRACE, that measures gravity field variations from which mass change is computed, shows equivalent seasonal mass loss fluctuations in summer and mass gain in winter with an overall negative trend. The simulated mass change rates resemble 98 % of GRACE's rate (see supplementary).

4.3 Ice surface elevation

$ISSM_{PT}$ simulates 20–100 % ice surface lowering from 1849 to 2012 over an area reaching 50 km upstream from the 2012 terminus. Transient surface elevation changes along the central flow lines of UI-1, UI-2 and UI-3 are visualised in movie01 (supplementary). The model simulation shows increased surface lowering in the time periods 1930/40, 1970/80 and from 2000 onwards.

Simulated surface elevation in 2005 lies within ±20 % of the observed surface elevation (GIMP) and in 2012 it lies within −20 and −10 % of observations (ArcticDEM). The 1985 DEM based on aerial photographs (Korsgaard et al., 2016) reaches at most 40 km inland. Simulated surface elevation is 60 to 100 % higher around UI-1 and UI-2 than the 1985 reconstruction and 10 % lower on average along UI-3.

NASA Operation IceBridge (Thomas and Studinger, 2010; Krabill, 2010, updated 2016) provides ice surface elevation along UI-1 (2009–2012) and UI-3 (1994, 1999, 2002, 2009, 2010, 2012). A mean value comparison along UI-3 flow lines (Figure 4), illustrate that the simulated surface elevation is two third of that observed 0–5 km upstream of the 2012 terminus and 56-62 % of that observed 5–10 km upstream of the 2012 terminus. Simulated surface elevations close to the UI-1 terminus resemble IceBridge observations to 90–100 %. Further upstream, UI-1 simulation results are 70–80 % of observed ice surface elevation. Observed IceBridge and simulated surface elevation along flow lines 5 km downstream and 20 km upstream of the 2012 terminus have high correlation with R-squared values of 0.93 for UI-1 and 0.97 for UI-3.

$ISSM_{PT}$ simulates trends in elevation that are equivalent to those of Kjær et al. (2012) and Khan et al. (2013) between 1985 and 2010 on UI-1 and UI-3, though not on UI-2. Note that the observed thinning south of UI-3 between 1985 and 1991 (Khan et al., 2013) is not reproduced in $ISSM_{PT}$.

The Cryosphere Discuss., https://doi.org/10.5194/tc-2017-121
Manuscript under review for journal The Cryosphere
Discussion started: 17 July 2017

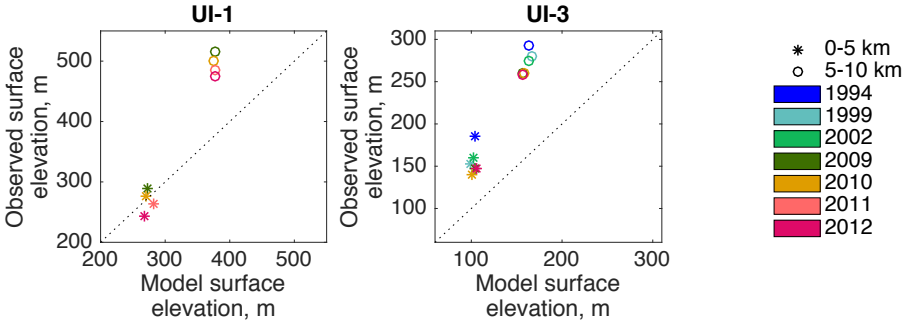

Figure 4. Observed vs. simulated ice surface elevation along flight lines (IceBridge surface elevation data; Thomas and Studinger, 2010; Krabill, 2010, updated 2016) over UI-1 and UI-3. Stars mark mean values between 0 and 5 km from the 2012 terminus, dots refer to mean values 5–10 km upstream. Flight lines over UI-1 are available for the years 2009, 2010, 2011, 2012 and over UI-3 in the years 1994, 1999, 2002, 2009, 2010, 2012.

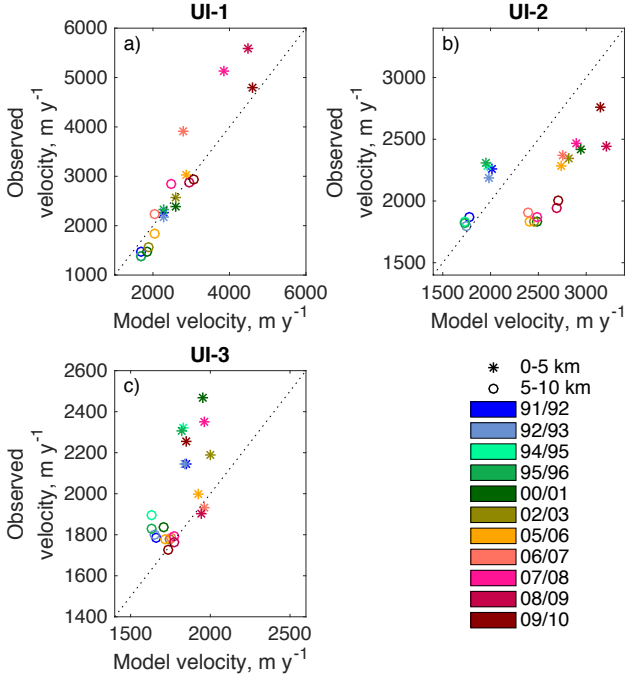

Figure 5. Observed vs. simulated ice surface velocities along the central flow lines of UI-1, UI-2 and UI-3. Stars mark mean velocities between 0 and 5 km from the 2012 terminus, dots refer to mean values 5–10 km upstream. Velocity data in the winters of 1991/92, 1992/93, 1994/95, 1995/96, 2002/03, 2005/06, 2006/07 and 2008/09 are provided by CCI (Nagler et al., 2017). Winter velocity maps from 2000/01, 2007/08 and 2009/10 are given by MEaSUREs (Howat, 2016).

The Cryosphere Discuss., https://doi.org/10.5194/tc-2017-121
Manuscript under review for journal The Cryosphere
Discussion started: 17 July 2017

4.4 Ice surface velocity

By the end of the $ISSM_{PT}$ simulation, ice flow velocities doubles at UI-1 and UI-2 and accelerates by 55 % at UI-3 compared to 1849. The simulated ice surface velocity evolution in plane view over the study period can be viewed in movie02 (supplementary). Short-term accelerations coincide with the induced ice mass change due to the prescribed terminus change (see movie01, supplementary). The simulation reproduces seasonal and annual velocity variations due to the SMB forcing in the model. Small (20 m y^{-1}) annual velocity fluctuations are forced by seasonal SMB fluctuations. Each retreat from the prescribed terminus change is followed by an acceleration between 1 and 70 % and 5–30 % surface lowering, lasting 0.5 to 6 months.

Simulated 2009 ice surface velocity is within ±20 % of observations from Rignot and Mouginot (2012), except in the shear margins, where simulated velocities are up to 200 % of observations. Winter velocity maps between 1991 and 2010 are used to evaluate recent changes in simulated velocity. Observed and simulated winter ice surface velocity averaged between 0 and 5 km and 5 to 10 km upstream of 2012 terminus (Fig. 5) have R-squared values of 0.90 on UI-1, 0.88 on UI-2 and 0.92 on UI-3. Observations show 20 % velocity increase on UI-1 from 07/08 to 08/09 not captured in $ISSM_{PT}$.

5 Discussion

The comparison of $ISSM_{PT}$ and $ISSM_{control}$ shows that the ice surface velocity and elevation are significantly affected by the prescribed marginal changes. After each prescribed terminus change, $ISSM_{PT}$ simulates short (0.5 to 6 months) periods of faster flow (1–70 % acceleration), and the surface elevation lowers up to 30 % at the new terminus in response to the ice flow acceleration. These are dynamic readjustments to instantly reduced terminal flow resistance from the prescribed retreat, which is induced in discrete time steps.

While $ISSM_{PT}$ produces maximum velocity and surface elevation changes of 275 % and 84 % respectively, $ISSM_{control}$ simulates minor changes (maximum ±7 %) in ice velocity and surface elevation, describing only changes in SMB. This highlights the importance of simulated terminus retreat in order to reproduce a UI glacial system evolution. In 1985–2012, $ISSM_{PT}$ simulates mass changes similar to observations (Kjær et al., 2012; Khan et al., 2013; Larsen et al., 2016) and ice surface elevation being within 20 % of GIMP or ArcticDEM and CCI or MEaSUREs velocity observations.

Recent studies suggest dividing mass balance into atmospheric and dynamically driven processes (Nick et al., 2009; Howat and Eddy, 2011; Kjær et al., 2012; Enderlin and Howat, 2013). Our simulation indicates three distinct MB periods when considering ΔSMB and ΔDIL. From the simulation start in 1849 to 1932, the total UI MB is the same for $ISSM_{control}$ and $ISSM_{PT}$, only diverging five times by one to four Gt y^{-1} when prescribed retreat is enforced. The increasing ΔSMB trend leads to a positive MB and thus mass gain. $ISSM_{PT}$ velocities start to differ from $ISSM_{control}$ following the first prescribed retreat in 1862, showing a short (< 1 month) acceleration. The simulation indicates stable glacier behaviour without dynamically caused acceleration or thinning.

From 1925 onwards, ΔSMB reveals a negative trend, initiating the negative MB trend that lasts until the simulation end in 2012. Between 1931 and 1992, in two instances (1931–1960 and 1960–1992), 5–7 year periods of sustained less-positive SMB are followed by approximately 20 year long periods of elevated ΔDIL.

The Cryosphere Discuss., https://doi.org/10.5194/tc-2017-121
Manuscript under review for journal The Cryosphere
Discussion started: 17 July 2017

Within this 60 years of simulation 31 terminus changes are prescribed, each removing 0.4–5 Gt of ice, which is as much as each of the five terminus changes the preceding 82 years (Fig. 2). The simulated mass loss in this period is therefore highly controlled by the prescribed retreat. ΔDIL consists of the removed ice mass at a prescribed retreat and of changes in ice mass flux caused by the acceleration of the glacier. We simulate two increased ΔDIL periods preceded by low ΔSMB as the result of observed terminus retreat. Induced by the prescribed terminus change in 1960 and 1966, a new period with increased ΔDIL lasts until 1992. UI's glaciers aim again for equilibrium, interrupted by seven prescribed terminus changes.

From 1999 onwards, ΔDIL and ΔSMB are roughly equivalent in contribution to the elevated negative MB. The simulation computes elevated dynamic ice loss due to 5.5 km terminus retreat on UI-1 within 12 years. We can not resolve, whether the increased retreat of UI-1 is due to (1) the change in ΔSMB from positive to negative values (+7 Gt to −7 Gt) or whether the glacier itself reaches an unstable position. However, as a result the retreat causes increased simulated ΔDIL adding up to the same amount as the increased negative ΔSMB. UI-2 shows similar behaviour. The result is a negative MB twice as negative as in any year before. In contrast, UI-3 is nearly stable, retreating 0.53 km between 1999 and 2012 and even advances in some years. It cannot be determined, whether UI-1 and UI-2 also reach a stable position soon or whether they will continue to retreat and accelerate.

The simulation reproduces not only the retreat, but also the observed terminus advances at UI-1 and UI-2 in summer 2012 and at UI-3 in the summers 2001, 2003 and 2007. However, MEaSUREs data indicate 20 % speed-up on UI-1 from 2007–2008 to 2008–2009, when a large floating ice tongue breaks off (Larsen et al., 2016). The observed acceleration is not captured by the simulation and may be related to unresolved loss in buttressing in the simulation.

6 Conclusions

Our study shows that glacier front changes are necessary for ice model simulations to reach realistic present day ice surface velocity and elevation. Prescribed terminus position change avoids calving and melt rate estimations and reduces simulated retreat uncertainty. Dynamic ice discharge is responsible for 80 % mass change in the 1985–2005 period and thereby plays an important role for UI's acceleration and thinning. $ISSM_{PT}$ captures distinct mass loss periods of dynamically driven ice mass loss and extends the periods discussed in Kjær et al. (2012) and Khan et al. (2013) from 1985 to 1932. The method is applicable to different glaciers and time periods, since we realistically reconstruct the 164 year UI glacial evolution matching observed velocity, surface elevation and mass changes within ±20 % of observations, without any further assumptions.

Our approach is limited, since it needs defined terminus position changes throughout the simulation period, and it cannot be used in future projections. However, simulation results show the importance of including calving into ice sheet models in order to capture velocity and thickness changes of a glacier. Better physically based calving laws are needed to understand and predict future glacier behaviour and glacier contribution to sea level rise. Our method can help evaluating calving laws during past simulations before applying them in future simulations. Short-term simulations with prescribed terminus position change might help answer the question, if seasonal terminus position variations are necessary to capture long-term glacier behaviour,

to determine what data is needed to evaluate and construct new calving laws. Future work could include comparisons with the physically based calving laws (e.g. Bondzio et al., 2016; Morlighem et al., 2016a) and application of our method to other tidewater glaciers.

Author contributions. K.H., N.J.S, E.Y.L., J.E.B., K.H.K., K.K.K. and S.H.L designed the study and setup the model. K.H. performed the study and data comparison and led the writing of the manuscript, in which she received support from all authors. M.M. created the bed geometry from bathymetry data. K.K.K. provided trimline data and observed terminus positions. A.M.S. processed winter ice surface velocity maps from ERS and ENVISAT.

Competing interests. The authors declare that they have no conflict of interest.

Acknowledgements. This study is part of the project "Multi-millennial ice volume changes of the Greenland Ice Sheet" funded by the Geocenter Danmark. KKK was supported by the Danish Council for Independent Research (DFF -4090-00151). We thank Brian Vinter and his team at Niels Bohr Institute, Copenhagen University, for generously supplying high performance computing resources. We acknowledge the use of bathymetry data provided by Eric Rignot and Todd Dupont, Department of Earth System Science, University of California-Irvine, USA, produced during a 2012 NASA campaign. The authors wish to thank Camilla Snowman Andresen, Geological Survey of Greenland and Denmark, for providing bathymetry measurements. Observed termini between 1999 and 2012 were provided by Trine Jensen and Karina Hansen, Geological Survey of Greenland and Denmark. We acknowledge and thank the Ice Sheet System Model group for producing and making available their model. We also acknowledge the use of the DEMs from GIMP, ArcticDEM and Niels Korsgaard and the velocity data provided by NASA, all available online.

References

Åström, J. A., Riikilä, T. I., Tallinen, T., Zwinger, T., Benn, D., Moore, J. C., and Timonen, J.: A particle based simulation model for glacier dynamics, The Cryosphere, 7, 1591–1602, doi:10.5194/tc-7-1591-2013, 2013.

Åström, J. A., Vallot, D., Schäfer, M., Welty, E. Z., O'Neel, S., Bartholomaus, T. C., Liu, Y., Riikilä, T. I., Zwinger, T., Timonen, J., and Moore, J. C.: Termini of calving glaciers as self-organized critical systems, Nature Geoscience, 7, 874–878, doi:10.1038/ngeo2290, 2014.

Andresen, C. S., Kjeldsen, K. K., Harden, B., Nørgaard-Pedersen, N., and Kjær, K. H.: Outlet glacier dynamics and bathymetry at Upernavik Isstrøm and Upernavik Isfjord, North-West Greenland, Geological Survey of Denmark and Greenland Bulletin, pp. 79–81, doi:10.5194/tc-10-1965-2016, 2014.

Benn, D. I., Warren, C. R., and Mottram, R. H.: Calving processes and the dynamics of calving glaciers, Earth Science Reviews, 82, 143–179, doi:10.1016/j.earscirev.2007.02.002, 2007.

Bevan, S. L., Luckman, A., and Murray, T.: Glacier dynamics over the last quarter of a century at Helheim, Kangerdlugssuaq and 14 other major Greenland outlet glaciers, Cryosphere, 6, 923–937, doi:10.5194/tc-6-923-2012, http://www.the-cryosphere.net/6/923/2012/, 2012.

Bondzio, J. H., Seroussi, H., Morlighem, M., Kleiner, T., Rückamp, M., Humbert, A., and Larour, E. Y.: Modelling calving front dynamics using a level-set method: application to Jakobshavn Isbræ, West Greenland, The Cryosphere, 10, 497–510, doi:10.5194/tc-10-497-2016, 2016.

Bondzio, J. H., Morlighem, M., Seroussi, H., Kleiner, T., Rückamp, M. Mouginot, J., Moon, T., Larour, E. Y., and Humbert, A.: The mechanisms behind Jakobshavn Isbræ's acceleration and mass loss: a 3D thermomechanical model study, Geophysical Research Letters, doi:10.1002/2017GL073309, 2017.

Box, J. E.: Greenland ice sheet mass balance reconstruction. Part II: Surface mass balance (1840-2010), Journal of Climate, 26, doi:10.1175/JCLI-D-12-00518.1, 2013.

Box, J. E., Bromwich, D. H., Veenhuis, B. A., Bai, L.-S., Stroeve, J. C., Rogers, J. C., Steffen, K., Haran, T., and Wang, S.-H.: Greenland Ice Sheet Surface Mass Balance Variability (1988 2004) from Calibrated Polar MM5 Output*, Journal of Climate, 19, 2783, doi:10.1175/JCLI3738.1, 2006.

Cook, S., Rutt, I. C., Murray, T., Luckman, A., Zwinger, T., Selmes, N., Goldsack, A., and James, T. D.: Modelling environmental influences on calving at Helheim Glacier in eastern Greenland, The Cryosphere, 8, 827–841, doi:10.5194/tc-8-827-2014, 2014.

Courant, R., Friedrichs, K., and Lewy, H.: On the Partial Difference Equations of Mathematical Physics, IBM J. Res. Dev., 11, 215–234, doi:10.1147/rd.112.0215, http://dx.doi.org/10.1147/rd.112.0215, 1967.

Cuffey, K. and Paterson, W.: The Physics of Glaciers, Elsevier Science, 2010.

Enderlin, E. M. and Howat, I. M.: Submarine melt rate estimates for floating termini of Greenland outlet glaciers (2000-2010), Journal of Glaciology, 59, 67–75, doi:10.3189/2013JoG12J049, 2013.

Fenty, A., Willis, J. K., Khazendar, A., Dinardo, S., Forsberg, R., Fukumori, I., Holland, D., Jakobsson, M., Moller, D., Morison, J., Münchow, A., Rignot, E., Schodlok, M., Thompson, A. F., Tinto, K., Rutherford, M., and Trenholm, N.: Oceans Melting Greenland: Early Results from NASA's Ocean-Ice Mission in Greenland, Oceanography, 29, doi:10.5670/oceanog.2016.100, 2016.

Gardner, A. S., Moholdt, G., Cogley, J. G., Wouters, B., Arendt, A. A., Wahr, J., Berthier, E., Hock, R., Pfeffer, W. T., Kaser, G., Ligtenberg, S. R. M., Bolch, T., Sharp, M. J., Hagen, J. O., van den Broeke, M. R., and Paul, F.: A Reconciled Estimate of Glacier Contributions to Sea Level Rise: 2003 to 2009, Science, 340, 852–857, doi:10.1126/science.1234532, 2013.

Howat, I. M.: MEaSURES Greenland Ice Velocity: Selected Glacier Site Velocity Maps from Optical Images, Version 2, doi:10.5067/EYV1IP7MUNSV, accessed: 2016-03-27, 2016.

Howat, I. M. and Eddy, A.: Multi-decadal retreat of Greenland's marine-terminating glaciers, Journal of Glaciology, 57, 389–396, doi:10.3189/002214311796905631, 2011.

Howat, I. M., Negrete, A., and Smith, B. E.: The Greenland Ice Mapping Project (GIMP) land classification and surface elevation data sets, The Cryosphere, 8, 1509–1518, doi:10.5194/tc-8-1509-2014, 2014.

Jensen, T. S., Box, J. E., and Hvidberg, C. S.: A sensitivity study of annual area change for Greenland ice sheet marine terminating outlet glaciers: 1999-2013, Journal of Glaciology, 62, 72–81, doi:10.1017/jog.2016.12, 2016.

Khan, S. A., KjæR, K. H., Korsgaard, N. J., Wahr, J., Joughin, I. R., Timm, L. H., Bamber, J. L., Broeke, M. R., Stearns, L. A., Hamilton, G. S., Csatho, B. M., Nielsen, K., Hurkmans, R., and Babonis, G.: Recurring dynamically induced thinning during 1985 to 2010 on Upernavik Isstrøm, West Greenland, Journal of Geophysical Research (Earth Surface), 118, 111–121, doi:10.1029/2012JF002481, 2013.

Khan, S. A., Aschwanden, A., Bjørk, A. A., Wahr, J., Kjeldsen, K. K., and Kjær, K. H.: Greenland ice sheet mass balance: a review, Reports on Progress in Physics, 78, 046801, doi:10.1088/0034-4885/78/4/046801, 2015.

Kjær, K. H., Khan, S. A., Korsgaard, N. J., Wahr, J., Bamber, J. L., Hurkmans, R., van den Broeke, M., Timm, L. H., Kjeldsen, K. K., Bjørk, A. A., Larsen, N. K., Jørgensen, L. T., Færch-Jensen, A., and Willerslev, E.: Aerial Photographs Reveal Late-20th-Century Dynamic Ice Loss in Northwestern Greenland, Science, 337, 569, doi:10.1126/science.1220614, 2012.

Kjeldsen, K. K., Korsgaard, N. J., Bjørk, A. A., Khan, S. A., Box, J. E., Funder, S., Larsen, N. K., Bamber, J. L., Colgan, W., van den Broeke, M., Siggaard-Andersen, M.-L., Nuth, C., Schomacker, A., Andresen, C. S., Willerslev, E., and Kjær, K. H.: Spatial and temporal distribution of mass loss from the Greenland Ice Sheet since AD 1900, nature, 528, 396–400, doi:10.1038/nature16183, 2015.

Korsgaard, N. J., Nuth, C., Khan, S. A., Kjeldsen, K. K., Bjørk, A. A., Schomacker, A., and Kjær, K. H.: Digital elevation model and orthophotographs of Greenland based on aerial photographs from 1978-1987, Nature Scientific Data, Volume 3, id. 160032 (2016)., 3, 160032, doi:10.1038/sdata.2016.32, 2016.

Krabill, W. B.: IceBridge ATM L2 Icessn Elevation, Slope, and Roughness. Version 2., doi:10.5067/CPRXXK3F39RV., accessed: 2016-06-10, 2010, updated 2016.

Larour, E., Seroussi, H., Morlighem, M., and Rignot, E.: Continental scale, high order, high spatial resolution, ice sheet modeling using the Ice Sheet System Model (ISSM), Journal of Geophysical Research (Earth Surface), 117, F01022, doi:10.1029/2011JF002140, 2012.

Larsen, S. H., Khan, S. A., Ahlstrøm, A. P., Hvidberg, C. S., Willis, M. J., and Andersen, S. B.: Increased mass loss and asynchronous behavior of marine-terminating outlet glaciers at Upernavik Isstrøm, NW Greenland, Journal of Geophysical Research (Earth Surface), 121, 241–256, doi:10.1002/2015JF003507, 2016.

Lea, J. M., Mair, D. W. F., Nick, F. M., Rea, B. R., van As, D., Morlighem, M., Nienow, P. W., and Weidick, A.: Fluctuations of a Greenlandic tidewater glacier driven by changes in atmospheric forcing: observations and modelling of Kangiata Nunaata Sermia, 1859-present, The Cryosphere Discussions, 8, 2005–2041, doi:10.5194/tcd-8-2005-2014, 2014.

MacAyeal, D. R.: Large-scale ice flow over a viscous basal sediment - Theory and application to ice stream B, Antarctica, Journal of Geophysical Research, 94, 4071–4087, doi:10.1029/JB094iB04p04071, 1989.

MacAyeal, D. R.: Binge/purge oscillations of the Laurentide Ice Sheet as a cause of the North Atlantic's Heinrich events, Paleoceanography, 8, 775–784, doi:10.1029/93PA02200, 1993.

McConnell, J. R., Lamorey, G., Hanna, E., Mosley-Thompson, E., Bales, R. C., Belle-Oudry, D., and Kyne, J. D.: Annual net snow accumulation over southern Greenland from 1975 to 1998, Journal of Geophysical Research: Atmospheres, 106, 33 827–33 837, doi:10.1029/2001JD900129, 2001.

McMillan, M., Leeson, A., Shepherd, A., Briggs, K., Armitage, T. W. K., Hogg, A., Kuipers Munneke, P., Broeke, M., Noël, B., Berg, W. J., Ligtenberg, S., Horwath, M., Groh, A., Muir, A., and Gilbert, L.: A high-resolution record of Greenland mass balance, Geophysical Research Letters, 43, 7002–7010, doi:10.1002/2016GL069666, 2016.

Moon, T., Joughin, I., Smith, B., Broeke, M. R., Berg, W. J., Noël, B., and Usher, M.: Distinct patterns of seasonal Greenland glacier velocity, Geophysical Research Letters, 41, 7209–7216, doi:10.1002/2014GL061836, 2014.

Morlighem, M., Rignot, E., Seroussi, H., Larour, E., Ben Dhia, H., and Aubry, D.: Spatial patterns of basal drag inferred using control methods from a full-Stokes and simpler models for Pine Island Glacier, West Antarctica, Geophysical Research Letters, 37, L14 502, doi:10.1029/2010GL043853, 2010.

Morlighem, M., Rignot, E., Seroussi, H., Larour, E., Ben Dhia, H., and Aubry, D.: A mass conservation approach for mapping glacier ice thickness, Geophysical Research Letters, 38, L19 503, doi:10.1029/2011GL048659, 2011.

Morlighem, M., Rignot, E., Mouginot, J., Seroussi, H., and Larour, E.: Deeply incised submarine glacial valleys beneath the Greenland ice sheet, Nature Geoscience, 7, 418–422, doi:10.1038/ngeo2167, 2014.

Morlighem, M., Bondzio, J., Seroussi, H., Rignot, E., Larour, E., Humbert, A., and Rebuffi, S.: Modeling of Store Gletscher's calving dynamics, West Greenland, in response to ocean thermal forcing, Geophysical Research Letters, 43, 2659–2666, doi:10.1002/2016GL067695, 2016a.

Morlighem, M., Rignot, E., and Willis, J. K.: Improving Bed Topography Mapping of Greenland Glaciers Using NASA's Oceans Melting Greenland (OMG) Data, Oceanography, 29, https://doi.org/10.5670/oceanog.2016.99, 2016b.

Motyka, R. J., Truffer, M., Fahnestock, M., Mortensen, J., Rysgaard, S., and Howat, I. M.: Submarine melting of the 1985 Jakobshavn Isbræ floating tongue and the triggering of the current retreat, Journal of Geophysical Research, 116, 1–17, doi:10.1029/2009JF001632, 2011.

Nagler, T., Forsberg, R., Marcus, E., and Hauglund, K.: Product User Guide (PUG) for the Greenland Ice Sheet cci project of ESA's Climate Change Initiative, version 2.1, http://www.esa-icesheets-greenland-cci.org/, 2017.

Nick, F. M., Vieli, A., Howat, I. M., and Joughin, I.: Large-scale changes in Greenland outlet glacier dynamics triggered at the terminus, Nature Geoscience, 2, 110–114, doi:10.1038/ngeo394, 2009.

Nick, F. M., van der Veen, C. J., Vieli, A., and Benn, D. I.: A physically based calving model applied to marine outlet glaciers and implications for the glacier dynamics, Journal of Glaciology, 56, 781–794, doi:10.3189/002214310794457344, 2010.

Nick, F. M., Vieli, A., Andersen, M. L., Joughin, I., Payne, A., Edwards, T. L., Pattyn, F., and van de Wal, R. S. W.: Future sea-level rise from Greenland's main outlet glaciers in a warming climate, nature, 497, 235–238, doi:10.1038/nature12068, 2013.

Noh, M.-J. and Howat, I. M.: Automated stereo-photogrammetric DEM generation at high latitudes: Surface Extraction with TIN-based Search-space Minimization (SETSM) validation and demonstration over glaciated regions, GIScience & Remote Sensing, 52, 198–217, doi:10.1080/15481603.2015.1008621, 2015.

O'Leary, M. and Christoffersen, P.: Calving on tidewater glaciers amplified by submarine frontal melting, Cryosphere, 7, 119–128, doi:10.5194/tc-7-119-2013, 2013.

OMG Mission.: Bathymetry (sea floor depth) data from the ship-based bathymetry survey. Ver. 0.1, doi:10.5067/OMGEV-BTYSS, dataset accessed: 2016-06-10, 2016.

Podrasky, D., Truffer, M., Fahnestock, M., Amundson, J., Cassotto, R., and Joughin, I.: Outlet glacier response to forcing over hourly to interannual timescales, Jakobshavn Isbræ, Greenland, Journal of Glaciology, 58, 1212–1226, doi:10.3189/2012JoG12J065, 2012.

Pritchard, H. D., Arthern, R. J., Vaughan, D. G., and Edwards, L. A.: Extensive dynamic thinning on the margins of the Greenland and Antarctic ice sheets, nature, 461, 971–975, doi:10.1038/nature08471, 2009.

Rignot, E. and Mouginot, J.: Ice flow in Greenland for the International Polar Year 2008-2009, Geophysical Research Letters, 39, L11 501, doi:10.1029/2012GL051634, 2012.

Rignot, E., Velicogna, I., van den Broeke, M. R., Monaghan, A., and Lenaerts, J. T. M.: Acceleration of the contribution of the Greenland and Antarctic ice sheets to sea level rise, Geophysical Research Letters, 38, L05 503, doi:10.1029/2011GL046583, 2011.

Rignot, E., Fenty, I., Xu, Y., Cai, C., Velicogna, I., Ó Cofaigh, C., Dowdeswell, J. A., Weinrebe, W., Catania, G. A., and Duncan, D.: Bathymetry data reveal glaciers vulnerable to ice-ocean interaction in Uummannaq and Vaigat glacial fjords, west Greenland, Geophysical Research Letters, 2014, 1–8, doi:10.1002/2016GL067832.Received, 2016.

Rosenau, R., Schwalbe, E., Maas, H.-G., Baessler, M., and Dietrich, R.: Grounding line migration and high-resolution calving dynamics of Jakobshavn Isbræ, West Greenland, Journal of Geophysical Research (Earth Surface), 118, 382–395, doi:10.1029/2012JF002515, 2013.

Schlegel, N.-J., Wiese, D. N., Larour, E. Y., Watkins, M. M., Box, J. E., Fettweis, X., and van den Broeke, M. R.: Application of GRACE to the assessment of model-based estimates of monthly Greenland Ice Sheet mass balance (2003-2012), The Cryosphere, 10, 1965–1989, doi:10.5194/tc-10-1965-2016, 2016.

Seroussi, H., Morlighem, M., Larour, E., Rignot, E., and Khazendar, A.: Hydrostatic grounding line parameterization in ice sheet models, The Cryosphere Discussions, 8, 3335–3365, doi:10.5194/tcd-8-3335-2014, 2014.

Thomas, R. and Studinger, M. S.: Pre-IceBridge ATM L2 Icessn Elevation, Slope, and Roughness, Version 1., doi:10.5067/6C6WA3R918HJ, accessed: 2016-06-10, 2010.

Todd, J. and Christoffersen, P.: Are seasonal calving dynamics forced by buttressing from ice mélange or undercutting by melting? Outcomes from full-Stokes simulations of Store Glacier, West Greenland, The Cryosphere, 8, 2353–2365, doi:10.5194/tc-8-2353-2014, 2014.

van As, D., Fausto, R. S., Cappelen, J., Van de Wal, R. S. W., Braithwaite, R. J., Machguth, H., and PROMICE project team: Placing Greenland ice sheet ablation measurements in a multi-decadal context, Geol. Surv. Denmark Greenland Bull, 35, 71–74, 2016.

van den Broeke, M., Bamber, J., Ettema, J., Rignot, E., Schrama, E., van de Berg, W. J., van Meijgaard, E., Velicogna, I., and Wouters, B.: Partitioning Recent Greenland Mass Loss, Science, 326, 984, doi:10.1126/science.1178176, 2009.

Velicogna, I., Sutterley, T. C., and van den Broeke, M. R.: Regional acceleration in ice mass loss from Greenland and Antarctica using GRACE time-variable gravity data, Geophysical Research Letters, 41, 8130–8137, doi:10.1002/2014GL061052, 2014.

Watkins, M. M., Wiese, D. N., Yuan, D.-N., Boening, C., and Landerer, F. W.: Improved methods for observing Earth's time variable mass distribution with GRACE using spherical cap mascons, Journal of Geophysical Research: Solid Earth, 120, 2648–2671, doi:10.1002/2014JB011547, 2015.

Weidick, A.: Frontal variations at Upernaviks Isstrøm in the last 100 years, Meddelser fra Dansk Geologisk Forening, 14, 52–60, 1958.

Wiese, D. N., Yuan, D.-N., Boening, C., Landerer, F. W., and Watkins, M. M.: JPL GRACE Mascon Ocean, Ice, and Hydrology Equivalent Water Height RL05M.1 CRI Filtered, Ver. 21, doi:10.5067/TEMSC-OLCR5, dataset accessed: 2015, 2015.